Effect of Ring Substituents on Formation Rates for Vanadium−Arene Clusters

Masaaki Hirano, Ken Judai, Atsushi Nakajima, and Koji Kaya*

Department of Chemistry, Faculty of Science and Technology, Keio University, 3-14-1 Hiyoshi, Kohoku-ku, Yokohama 223, Japan

Received: February 11, 1997; In Final Form: April 30, 1997[⊗]

Vanadium−arene complexes, $V_n(arene)_m$ (arene = benzene (C_6H_6), toluene ($C_6H_5CH_3$), and fluorobenzene (C_6H_5F)), were synthesized by the reaction of laser-vaporized vanadium atoms with arene vapor. Both the analysis of the mass spectra and the measurements of their ionization energies indicate that both $V_n(C_6H_5CH_3)_m$ and $V_n(C_6H_5F)_m$ clusters take a multiple-decker sandwich structure similar to the structure of $V_n(C_6H_6)_m$ clusters. The relative reactivity between benzene and toluene toward vanadium was also determined; toluene is 4 times as reactive as benzene for $V_1(C_6H_5CH_3)_1/V_1(C_6H_6)_1$ production and 2 times for $V_1(C_6H_5CH_3)_2/V_1(C_6H_6)_2$ production because of reactivity enhancement of the electron-donating ring substituent. In the case of the $V_n(C_6H_5F)_m$ cluster, it is found that the electron-withdrawing ring substituent of fluorobenzene results in much less reactivity than is observed for benzene and toluene.

1. Introduction

Since the advent of the laser vaporization method, transition metal clusters have been studied in the gas phase under molecular beam conditions, since they cannot be efficiently produced by a crucible method because of their high boiling temperatures. Several groups have independently succeeded in the synthesis of metal−molecular complexes in the gas phase to investigate the interaction between a metal atom and ligand molecules without the influence of a solvent. This has been done by modifying the laser vaporization method.[1−9]

Very recently, we have reported the preparation of metal−benzene multinuclear complexes, $M_n(C_6H_6)_m$, by the reaction of laser-vaporized metal atoms, M, with benzene vapor (M = V,[10] Co,[11] and other first-row transition metal atoms[12]). Reactivity of metal clusters, M_n, toward benzene has been found to differ widely, associated with selectively different skeleton structures.[12] Early transition metal atoms of scandium (Sc), titanium (Ti), and vanadium (V) form multiple-decker sandwich clusters, $M_n(C_6H_6)_m$ with $m = n - 1$, $m = n$, and $m = n + 1$ species, where metal atoms and benzene molecules are alternately piled up. On the other hand, the late transition metals of cobalt (Co) and nickel (Ni) prefer metal cluster complexes in which benzene molecules cover the M_n clusters. In the mass spectrum of $Co_n(C_6H_6)_m$ and $Ni_n(C_6H_6)_m$, every number of metal atoms (n) has a specific maximum number of benzene molecules adsorbed (m_{max}). These two types of the geometries can be well rationalized by (1) the 18-electron rule[13] and (2) the difference in the sequential dehydrogenation reactivity toward benzene between early and late transition metal clusters.[12] Since the complex between the late transition metal atom and two benzene molecules, $M_1(C_6H_6)_2$, has more than 18 electrons, the multiple-decker sandwich structure is unfavorable for the late transition metals, resulting in deformation into a bent form.[14] Furthermore, the early transition metal clusters (Sc_n, Ti_n, and V_n) can dehydrogenate benzene molecules[15] and give a variety of dehydrogenated products that are distributed over a wide mass range. In accordance with that, only the sandwich complexes were clearly observed in the mass spectra. On the other hand, the late transition metal clusters (Co_n and Ni_n)[16,17] cannot dehydrogenate benzene molecules. Thus, reaction with benzene leads to products of a specific composition; for example, trimer and tetramer take 3 and 4 benzene molecules at maximum, respectively. Among these metal−benzene clusters, it has been found that vanadium atoms can preferentially form larger multiple-decker sandwich clusters up to six layers.[10,12] This is reasonably explained by the fact that the system of vanadium−benzene multiple-decker sandwich compounds can conserve spin multiplicity during the reaction of the sandwich cluster formation.[18]

Since the discovery of ferrocene, $Fe(\eta^5\text{-}C_5H_5)_2$, in 1951,[19] organometallic compounds have attracted a lot of interest and have been investigated considerably both experimentally and theoretically to learn about metal−molecule interactions.[20−24] A metal atom interacts with aromatic molecules and often forms stable complexes through overlap of the ring π and π^* orbitals with appropriate orbitals of the metal atom(s).[25] The sandwich compound has a structure where a metal atom is located between two aromatic hydrocarbons such as the cyclopentadienyl radical, benzene, cyclooctatetraene, and so on.[20,26] Among the sandwich complexes between first-row transition metal atoms and benzene, $Cr(C_6H_6)_2$ is well-known to be stable in bulk because of the electronic structure having an 18-electron closed shell.[21] And also, $V(C_6H_6)_2$ and $Ti(C_6H_6)_2$ have been synthesized in bulk, although they lack 1 or 2 electrons of 18 electrons.

$V(C_6H_6)_2$ was first prepared in 1957 by the Fischer−Hafner method, i.e., the reduction of VCl_4 with $AlCl_3$/Al in refluxing arene followed by hydrolysis.[27] It was determined by EPR spectroscopy in an Ar matrix[28] to have a sandwich structure. Apart from the above Ti−, V−, and Cr−$(C_6H_6)_2$, other sandwich complexes consist of alkyl ring substituents, and other first-row transition metal complexes are known, such as Sc(1,3,5-tri-*tert*-butylbenzene)$_2$[29] and Fe(hexamethylbenzene)$_2$.[30] In this paper, we synthesized $V_n(arene)_m$ clusters (arene = benzene (C_6H_6), toluene ($C_6H_5CH_3$), and fluorobenzene (C_6H_5F)) by using the molecular beam method in combination with laser vaporization and a flow tube reactor. Then we discuss the difference in the reactivity of arene molecules toward vanadium atoms in order to clarify the effects of electron-donating and -withdrawing ring substituents on the η-bonded organometallic compounds.

* To whom correspondence should be addressed.

[⊗] Abstract published in *Advance ACS Abstracts,* June 1, 1997.

S1089-5639(97)00537-9 CCC: $14.00

2. Experimental Section

Details of the experimental setup have been provided elsewhere.[10] The $V_n(\text{arene})_m$ clusters were synthesized by a combination of the laser vaporization method with a flow-tube reactor. First, vanadium atoms were vaporized by irradiation with the second harmonic of a pulsed Nd^{3+}:YAG laser (532 nm), and the vaporized hot vanadium atoms were cooled to around room temperature by a pulse of He carrier gas (10 atm stagnation pressure). Then the metal atoms were sent into the flow-tube reactor, where arene (C_6H_6, $C_6H_5CH_3$, and/or C_6H_5F) vapor seeded in He gas (1−2 atm) was injected in synchronization with the flowing of the metal atoms. After skimming of the cluster beam, $V_n(\text{arene})_m$ clusters were ionized by an ArF excimer laser (193 nm; 6.42 eV) or the second harmonic of a dye laser pumped by an XeCl excimer laser. The photoions were mass-analyzed by a time-of-flight (TOF) mass spectrometer with reflectron.

Using the second harmonic of the dye laser, we determined ionization energies (E_is) of the $V_n(\text{arene})_m$ clusters through the measurement of photoionization efficiency curves. The photon energy was changed at a 0.01−0.03 eV interval in the range 5.95−3.50 eV, while the abundance and composition of the clusters were monitored by the ionization of the ArF laser. The fluences of the photoionization laser light were kept at ∼200 μJ/cm^2 to avoid multiphoton processes. To obtain photoionization efficiency curves, the ion intensities by the second harmonic of the tunable UV dye laser (I_{dye}) were plotted as a function of the photon energies with normalization to both the laser fluence (F_{dye} and F_{ArF}) and the ion intensities by ArF ionization (I_{ArF}). Then the normalized ion intensity, I, is obtained as follows:

$$I = \frac{I_{\text{dye}}}{F_{\text{dye}}} \frac{F_{\text{ArF}}}{I_{\text{ArF}}} \qquad (1)$$

The E_is of the clusters were determined from the extrapolation of the final decline in the photoionization efficiency curves. The uncertainty of the E_is was estimated to be typically ±0.05 eV.

The relative reactivity of arene molecules toward the vanadium atom was also measured. By the adustment of the laser fluence for vaporization, the V atom beam was generated, which was monitored by the mass distribution of V^+ cations. From the sample nozzle, we added the mixed arene gas, which was prepared by liquid mixtures of benzene−toluene with several different molar ratios. To know the partial pressure ratio in the injected gas, the mixed vapors were expanded from the nozzle and ionized by the second harmonic of the dye laser through a two-photon process via the S_1 state. The ratios of the ion intensity of benzene to that of toluene were plotted as a function of the molar ratios of the prepared liquid mixture, and then the partial pressure ratios in the molecular beam were determined. To estimate the relative reactivities of vanadium−arene compounds, ion intensity ratios of $V_1(C_6H_6)_1/V_1(C_6H_5CH_3)_1$ and $V_1(C_6H_6)_2/V_1(C_6H_5CH_3)_2$ in the ArF ionization mass spectra were measured as a function of the partial pressure ratios of benzene to toluene. With the same method, we also measured the relative reactivity of fluorobenzene to benzene toward vanadium atoms.

3. Results and Discussion

3.1. Mass Spectrum of the $V_n(\text{arene})_m$ Clusters. Parts a−c of Figure 1 show the typical mass spectra of the $V_n(C_6H_6)_m$,[10] $V_n(C_6H_5CH_3)_m$, and $V_n(C_6H_5F)_m$ clusters, respectively, produced by the above-described procedure. The peaks are labeled according to the notation (n, m), denoting the number of vanadium atoms (n) and arene molecules (m). In the photoionization mass spectra, the ion intensities would reflect the abundance of clusters, assuming that their E_is are lower than the photon energy of the ionization laser (6.42 eV) and that fragmentation is negligible. As discussed later, the E_is of the $V_n(\text{arene})_m$ clusters are below 6.42 eV. Since their mass abundance does not depend on the wavelength at about 6.42 and 5.9 eV except for $V_1(C_6H_5F)_2$, it may fairly be presumed that the ion intensities of the respective V_n $(\text{arene})_m$ clusters in Figure 1, except for $V_n(C_6H_5F)_m$, should reflect the abundance of the neutral clusters. Thus, the prominent peaks can be regarded as the abundant and stable clusters, although $V_1(C_6H_5F)_2$ might be more abundant. These three spectra were taken under the condition of a relatively high concentration of arene vapors. Even when this concentration was increased, the mass spectra remained unchanged. Therefore, the concentration of arene used is high enough to get final arene complexes toward metal vapors.

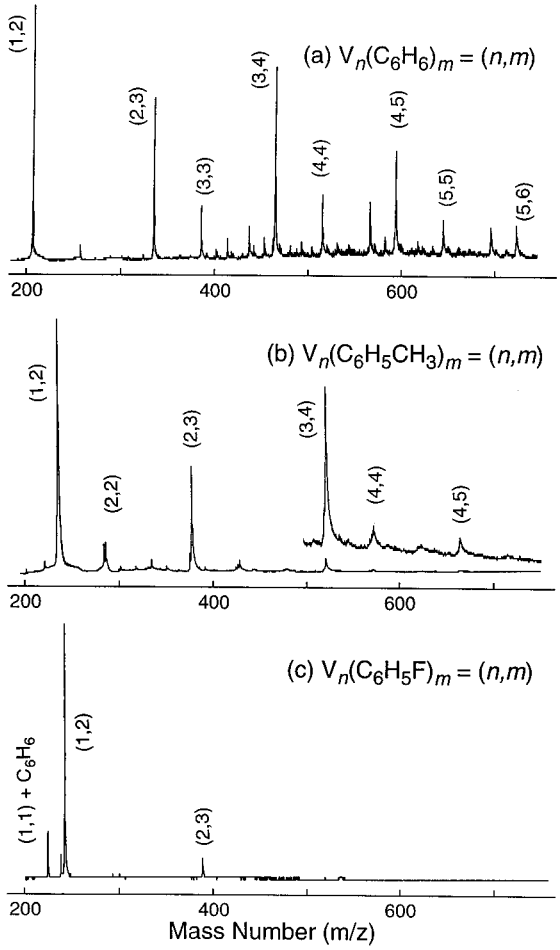

Figure 1. Time-of-flight mass spectra of $V_n(\text{arene})_m$ clusters; (a) $V_n(C_6H_6)_m$ (taken from ref 10); (b) $V_n(C_6H_5CH_3)_m$; (c) $V_n(C_6H_5F)_m$. Peaks of the clusters are labeled according to the notation (n, m) denoting the number of vanadium atoms n and arene molecules m.

As mentioned before, the organometallic clusters can take two types of structures. One is the multiple-decker sandwich structure in which metal atoms and arene molecules are alternately piled up as in $V_n(C_6H_6)_m$,[10] and the other is a structure in which the metal clusters are fully surrounded by arene molecules as in $Co_n(C_6H_6)_m$.[12] In parts a and b of Figure 1, the main products are $V_n(C_6H_6)_{n+1}$ ($n = 1-5$) and $V_n(C_6H_5CH_3)_{n+1}$ ($n = 1-4$), respectively, which are hereafter denoted as (n, $n + 1$). It seems reasonable to say that compositions of prominent peaks in these two mass spectra are almost the same. Therefore, the geometric structure of the $V_n(C_6H_5CH_3)_m$ cluster is reason-

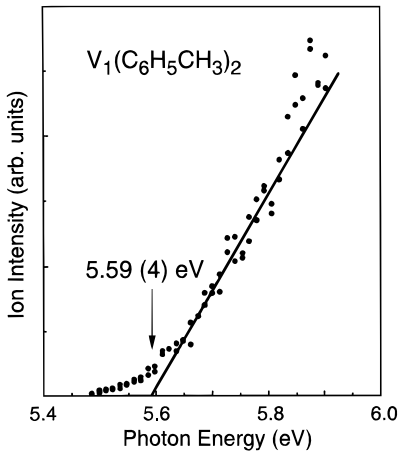

Figure 2. Photoionization efficiency curve of the $V_1(C_6H_5CH_3)_2$ cluster normalized to the power of the ionization laser. The photon energy was changed at 0.015 eV intervals in the range 5.85−5.50 eV. From the final decline of the curve, the E_i of the cluster was determined to be 5.59 ± 0.04 eV.

TABLE 1: Ionization Energies of $V_n(arene)_m$ Clusters in eV

	composition		
cluster	*n*	*m*	E_i[a]
$V_n(C_6H_5CH_3)_m$	1	1	5.30(6)
	1	2	5.59(4)
	2	2	5.25(6)
	2	3	4.66(5)
	3	3	4.50(6)
	3	4	4.16(5)
$V_n(C_6H_5F)_m$	1	2	5.92(5)
	2	3	5.02(5)

[a] Values in parentheses indicate experimental uncertainty; 5.30(6) represents 5.30 ± 0.06.

ably presumed to be the same multiple-decker sandwich as the $V_n(C_6H_6)_m$ cluster. In the case of $V_n(C_6H_5F)_m$ clusters in Figure 1c, only a few can be synthesized; the conspicuous products are $(n, m) = (1, 2)$ and $(2, 3)$. This is probably because the formation rate for $V_n(C_6H_5F)_m$ is low compared to $V_n(C_6H_6)_m$ and $V_n(C_6H_5CH_3)_m$. Since a long series of $(n, n + 1)$ compositions is one evidence for a sandwich cluster, we could not conclude whether $V_n(C_6H_5F)_m$ clusters may take multiple-decker sandwich structures or not.

3.2. Ionization Energies and Structure of $V_n(arene)_m$ Clusters. To obtain information about the electronic structures of $V_n(arene)_m$ clusters, their ionization energies, E_is, were measured using a photoionization spectroscopic method. The size dependence of E_i values of organometallic clusters differs much between the two types of structures.[10,11] For the multiple-decker sandwich cluster such as $V_n(C_6H_6)_m$, the E_i values decrease drastically with the cluster size.[10] On the other hand, for the M_n clusters fully covered with benzene molecules, such as $Co_n(C_6H_6)_m$, such a drastic decrease of E_is is never observed.[11,12] Figure 2 shows the photoionization efficiency (PIE) curve of $V_1(C_6H_5CH_3)_2$. As shown in Figure 2, the E_i of $V_1(C_6H_5CH_3)_2$ was determined to be 5.59 ± 0.04 eV from the extrapolation of the final decline of the ion intensities as a function of the photon energy. The E_i values of the $V_n(C_6H_5CH_3)_m$ and $V_n(C_6H_5F)_m$ determined by the same method are listed in Table 1. Figure 3 shows these E_i values plotted against the number of vanadium atoms, together with E_is of $V_n(C_6H_6)_m$.[10]

3.2.a. $V_n(C_6H_5CH_3)_m$ Clusters. The E_i size dependence of $V_n(C_6H_5CH_3)_m$ is strikingly similar to that of $V_n(C_6H_6)_m$; the E_i values decrease greatly as *n* is increased. This reason is

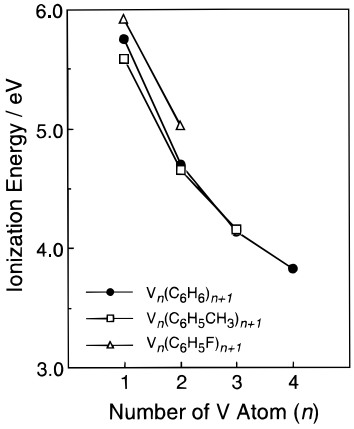

Figure 3. Dependence of E_is of $V_n(arene)_m$ clusters on the number of metal atoms. Solid circles, open squares, and open triangles denote E_is of $V_n(C_6H_6)_m$, $V_n(C_6H_5CH_3)_m$, and $V_n(C_6H_5F)_m$, respectively. E_is of $V_n(C_6H_6)_m$ are taken from ref 8.

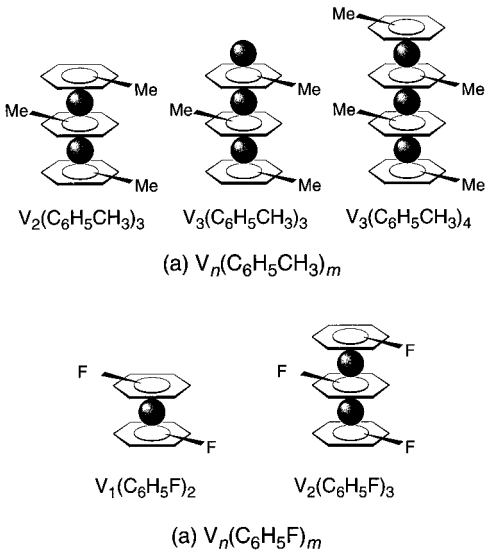

Figure 4. Proposed structures of (a) $V_n(C_6H_5CH_3)_m$ and (b) $V_n(C_6H_5F)_m$ clusters.

rationalized by the delocalization of d electrons of vanadium atoms along the molecular axis through interaction of π electrons on aromatic rings with the growth of the layered sandwich complexes.[10,11] Although theoretical investigations for this drastic E_i decrease have been in progress, it still remains an open question. As expected, since the E_i value of toluene (8.82 eV) is 0.43 eV lower than that of benzene (9.25 eV),[31] the E_i of $V_1C_6H_5CH_3)_2$ is 0.16 eV lower than that of $V_1(C_6H_6)_2$. This difference comes to be zero within experimental uncertainties when the number of vanadium atom is increased to $n = 3$. Because the ionization of the $V_n(arene)_{n+1}$ multiple-decker sandwich cluster occurs from nonbonding orbitals that come from 3d orbitals of the metal atoms, their electronic structures presumably become similar with increasing size of the sandwich cluster. From both the stable clusters in the mass spectra and the E_i decrement with *n*, it should be concluded that $V_n(C_6H_5CH_3)_m$ is the same as $V_n(C_6H_6)_m$ in both geometrical and electronic structures and takes the multiple-decker sandwich structure as shown in Figure 4a. To obtain information on the proposed sandwich structure, an experiment of infrared absorption is in progress in our group.

3.2.b. $V_n(C_6H_5F)_m$ Clusters. For $V_n(C_6H_5F)_m$ clusters, their E_is are a little higher than those of $V_n(C_6H_6)_m$ and $V_n(C_6H_5CH_3)_m$ (see Figure 3 and Table 1). Although the E_i of the fluorobenzene molecule (9.20 eV) is almost equal to that of

benzene (9.25 eV),[31] the E_i of $V_1(C_6H_5F)_2$ is higher than that of $V_1(C_6H_6)_2$ by 0.17 eV, and this difference is increased to 0.28 eV at a cluster size of $(n, m) = (2, 3)$. Along with only a few products of $V_n(C_6H_5F)_m$ clusters in the ArF mass spectra (see Figure 1c), the geometrical structure of the $V_n(C_6H_5F)_m$ cluster causes controversial discussion, but it may be deduced that the cluster takes the sandwich structure as shown in Figure 4b from the following three reasons: (i) the E_i of $V_1(C_6H_5F)_2$ is still very low, similar to that of other sandwich $M_1(arene)_2$ complexes;[32] (ii) the drastic decrease of E_is with the cluster size can also be found; (iii) in bulk, $V_1(C_6H_5F)_2$ has been prepared by the metal vapor synthesis in high yield.[33] In the case of $Cr_1(arene)_2$, E_is obtained by ultraviolet photoelectron spectroscopy indeed show a tendency similar to that of $V_1(arene)_2$ in this work: 5.40, 5.31, and 5.91 eV for $Cr_1(C_6H_6)_2$, $Cr_1(C_6H_5CH_3)_2$, and $Cr_1(C_6H_5F)_2$, respectively.[34] Furthermore, a single-crystal X-ray structure study for $V_1(p\text{-}C_6H_4F_2)_2$ has been made, indicating that it takes the sandwich structure.[35]

Unlike the neutrals, the $V_1(C_6H_5F)_2^-$ anion has been formed, while the $V_1(C_6H_6)_2^-$ anion has never been found irrespective of the satisfaction of the 18 valence electrons rule. An electrochemical study[36] has shown that $V_1(C_6H_6)_2$ has a negative electron affinity (EA), and our recent work indicates that this is because the occupied orbital by the excess electron is characteristic of nonbonding (d_{z^2}).[37] Since the EAs of benzene and fluorobenzene are similar, -1.15 and -0.89 eV,[38] $V_1(C_6H_5F)_2$ having the sandwich structure should have a negative EA as well as $V_1(C_6H_6)_2$. One possible explanation for the production of $V_1(C_6H_5F)_2^-$ is the structural deformation by electron attachment to $V_1(C_6H_5F)_2$, although the deformed structure cannot be clear. It seems preferable that the bond between V and F atoms is formed because the excess charge is distributed around the F−C bond in the fluorobenzene molecule because of the large electronegativity of an F atom. In fact, the photoelectron spectrum of $V_1(C_6H_5F)_1^-$ is strikingly different from those of $V_1(C_6H_6)_1^-$ and $V_1(C_6H_5CH_3)_1^-$, suggesting that the coordinate of fluorobenzene to the V atom is different from those of benzene and toluene in their anions.[37] Moreover, the vanadium fluoride anion, VF^-, and its arene complex are abundantly observed in the mass spectrum of the $V_n(C_6H_5F)_m^-$ anions. Therefore, the F atom in fluorobenzene is reasonably expected to work as a bonding site to V atoms in addition to the aromatic benzene ring. Namely, the $V_1(C_6H_5F)_2^-$ anion presumably takes a different structure from the sandwich structure of the neutral $V_1(C_6H_5F)_2$.

3.3. Reactivity of $V_1(arene)_1$ and $V_1(arene)_2$ Clusters. We investigated relative reactivity among benzene, toluene, and fluorobenzene molecules toward vanadium atoms to know the effect of electron-donating and -withdrawing ring substituents on the sandwich compounds. Figure 5 shows a mass spectrum of $V_n(C_6H_6)_m(C_6H_5CH_3)_l$ cluster when the vapor pressure of benzene and toluene is nearly equal. At a glance, one can see that ion intensities of $V_n(C_6H_5CH_3)_m$ clusters are larger than those of $V_n(C_6H_6)_m$ clusters. In the measurement of their relative production efficiency, we prepared mixed solution of benzene and toluene with several different molar ratios.

At first, we examined the partial pressures of benzene and toluene obtained from the mixed solution. Although it is well-known that benzene and toluene behave as nearly an ideal solution, it provides no sufficient guarantee against the partial pressures in the injected gas being the same as those determined by the treatment of the ideal solution because adsorption of arene molecules inside the tubing and the nozzle may change the partial pressures. The vapor of the mixture seeded in He gas was expanded from the nozzle and ionized by the second

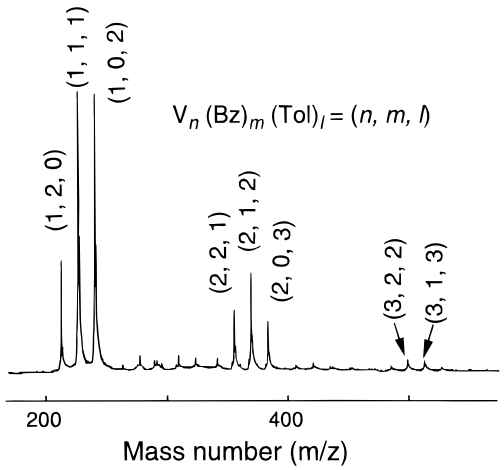

Figure 5. Time-of-flight mass spectra of $V_n(C_6H_6)_m(C_6H_5CH_3)_l$ clusters under almost equal partial pressures of benzene and toluene. Peaks of the clusters are labeled according to the notation (n, m, l) donating the number of vanadium atoms n, benzene m, and toluene molecules l.

harmonic of the dye laser through a two-photon process via the S_1 state. The ion intensity of each molecule, I_A (A = Bz (benzene) and Tol (toluene)), is expressed as a product of partial pressure (P_A), an ionization cross section (Φ_A), and the square of the ionization laser fluence (L_A); $I_A = P_A\Phi_A L_A^2$. We measured the dependence of ion intensity against the ionization laser fluence and made sure that ionization of benzene and toluene occurs through the two-photon process. Here, Φ_A does not depend on mixture ratios, so it can be expressed with the values for the pure sample (Bz or Tol) as follows:

$$\Phi_A = \frac{I_A^*}{((L_A^*)^2 P_A^*)} \tag{2}$$

where a notation with an asterisk means the value for the pure sample and P_{Tol}^* and P_{Bz}^* are vapor pressures of toluene and benzene obtained from the pure liquid, respectively. $P_{Tol}^* = 21.58$ Torr and $P_{Bz}^* = 75.59$ Torr at 293 K.[39] Therefore, the partial pressure ratio of benzene to toluene in a molecular beam, P_{Bz}/P_{Tol}, is expressed as follows:

$$\frac{P_{Bz}}{P_{Tol}} = \frac{I_{Bz}}{I_{Tol}} \frac{L_{Tol}^2}{L_{Bz}^2} \frac{\Phi_{Tol}}{\Phi_{Bz}}$$

$$= \frac{I_{Bz}}{I_{Tol}} \frac{L_{Tol}^2}{L_{Bz}^2} \frac{I_{Tol}^*/(L_{Tol}^{*2} P_{Tol}^*)}{I_{Bz}^*/(L_{Bz}^{*2} P_{Bz}^*)} \tag{3}$$

To ensure the above relationship, the partial pressure ratio (P_{Bz}/P_{Tol}) determined by eq 3 was plotted as a function of molar ratios (x_{Bz}/x_{Tol}) of the prepared liquid mixture, as shown in Figure 6. The plots can be fitted by a straight line having a slope of 3.7 ± 0.2.

When this relation was reasonably understood by Raoult's law that the vapor pressure of a component is proportional to its mole fraction in the liquid for an ideal solution,[40] a ratio of benzene vapor pressure to toluene (P_{Bz}/P_{Tol}) obtained from the liquid mixture can be written as

$$\frac{P_{Bz}}{P_{Tol}} = \frac{P_{Bz}^*}{P_{Tol}^*} \frac{x_{Bz}}{x_{Tol}} \tag{4}$$

where x_{Bz} and x_{Tol} are the mole fractions of benzene and toluene in the liquid mixture, respectively. Raoult's law indicates that

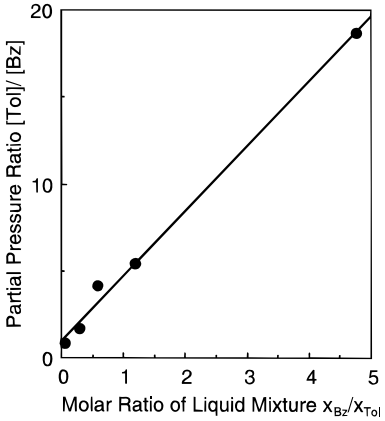

Figure 6. Plot of the partial pressure ratios of benzene to toluene vs molar ratios of prepared liquid mixtures. Partial pressure ratios were determined by ion intensity ratios via the two-photon process and eq 3 (see text). This straight line corresponds to Raoult's law, and indeed, the slope of 3.7 ± 0.2 is nearly equal to 3.5 of the ratio of vapor pressure of pure benzene to that of pure toluene, P_{Bz}^*/P_{Tol}^*, at 293 K (see text). It is safe to say that the vertical axis represents the partial pressure ratios of benzene to toluene.

the slope in Figure 6 should be equal to P_{Bz}^*/P_{Tol}^* if the expression for P_{Bz}/P_{Tol} in eq 3 is valid. Actually, the slope of 3.7 ± 0.2 is nearly equal to 3.50 of P_{Bz}^*/P_{Tol}^* at 293 K.[31] Therefore, it is safe to say that the vertical axis in Figure 6 represents the partial pressure ratios of benzene to toluene.

Next we measured the relative reactivity of benzene to toluene toward V atoms in the formation of $V_1(C_6H_6)_1$ and $V_1(C_6H_5CH_3)_1$. The reaction proceeds as follows:

$$V + Bz \xrightarrow{k_{Bz}} V_1(Bz)_1 \tag{5}$$

and

$$V + Tol \xrightarrow{k_{Tol}} V_1(Tol)_1 \tag{6}$$

Because the formation of $V_1(arene)_1$ is described as $(d[V_1(arene)_1])/dt = k_A[V][arene]$ (A = Bz and Tol), the concentration ratio of $[V_1(C_6H_5CH_3)_1]$ to $[V_1(C_6H_6)_1]$ is written as follows:

$$\frac{[V_1(Tol)_1]}{[V_1(Bz)_1]} = \frac{k_{Tol}}{k_{Bz}}\frac{[Tol]}{[Bz]} \tag{7}$$

The $V_n(arene)_m$ clusters were ionized through a one-photon process by an ArF excimer laser. The ion intensity of $V_1(arene)_1$ (I_{VA}; VA = VBz or VTol) is expressed as a product of an ionization cross section (Φ_{VA}), the ionization laser fluence (L_{VA}), and a concentration of $V_1(arene)_1$ ($[V_1(arene)_1]$); $I_{VA} = \Phi_{VA}L_{VA}[V_1(arene)_1]$. We can reasonably assume that the ionization cross sections for $V_1(C_6H_5CH_3)_1$ and $V_1(C_6H_6)_1$ are equal because (i) as mentioned above, ionization of the sandwich compounds occurs from nonbonding orbitals that come from metal 3d orbitals and their ionization energies are almost the same and (ii) the total absolute ionization cross sections for benzene and toluene by electron impact are almost the same at an impact energy from 20 to 250 eV; 5.704×10^{-16} cm^2 and 4.952×10^{-16} cm^2 at 30 eV, 10.799×10^{-16} cm^2 and 12.744×10^{-16} cm^2 at 50 eV, and so on.[41] Almost the same ionization cross section by electron impact means that the probability of direct ionization of benzene and toluene molecules differs little, although the absolute photoionization cross section for toluene has never been reported to our knowledge. Then it implies that the cross sections for ionization of $V_1(C_6H_6)_1$ and $V_1(C_6H_5CH_3)_1$ are expected to be almost the same.

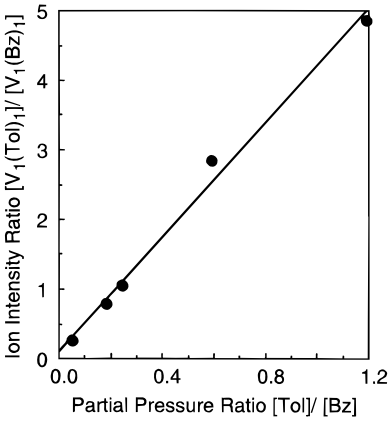

Figure 7. Plot of ion intensity ratios of $V_1(C_6H_5CH_3)_1$ to $V_1(C_6H_6)_1$ normalized to the laser fluence vs partial pressure ratios [Tol]/[Bz] in the molecular beam determined from eq 2. This straight line corresponds to eq 7 (see text). Assuming that ionization cross sections for both compounds were equal, the fitted slope of 4.1 ± 0.2 means k_T/k_B; that is, the reactivity of toluene toward a vanadium atom is 4 times larger than that of benzene.

Accordingly, ion intensity ratios between $V_1(C_6H_6)_1$ and $V_1(C_6H_5CH_3)$ normalized with the laser fluence mean the concentration ratios between $V_1(C_6H_6)_1$ and $V_1(C_6H_5CH_3)_1$ in the beam. In Figure 7, ion intensity ratios of $V_1(C_6H_6)_1$ to $V_1(C_6H_5CH_3)_1$ normalized with the laser fluence are plotted against partial pressure ratios [Tol]/[Bz] in the molecular beam determined from eq 3. The plot gives a straight line, and the slope of 4.1 ± 0.2 in Figure 7 corresponds to k_{Tol}/k_{Bz} as expressed by eq 7. Namely, the reactivity of toluene toward a vanadium atom is 4 times larger than that of benzene.

Finally, relative reactivity of toluene and benzene for $V_1(C_6H_5CH_3)_2$ and $V_1(C_6H_6)_2$ production has been determined by a similar method. The production reaction is expressed as follows:

$$V_1(Tol)_1 + Tol \xrightarrow{k_{VT-T}} V_1(Tol)_2 \tag{8}$$

and

$$V_1(Bz)_1 + Bz \xrightarrow{k_{VB-B}} V_1(Bz)_2 \tag{9}$$

The concentration ratios of the complexes in the beam, $[V_1(Tol)_2]/[V_1(Bz)_2]$, can be expressed in the following, assuming both clusters have the same ionization efficiency:

$$\frac{[V_1(Tol)_2]}{[V_1(Bz)_2]} = \frac{k_{VT-T}}{k_{VB-B}}\frac{[V_1(Tol)_1]}{[V_1(Bz)_1]}\frac{[Tol]}{[Bz]}$$

$$= \frac{k_{VT-T}}{k_{VB-B}}\frac{k_T}{k_B}\frac{[Tol]^2}{[Bz]^2} \tag{10}$$

In Figure 8, the ion intensity ratios of $V_1(C_6H_5CH_3)_2$ to $V_1(C_6H_6)_2$ normalized to the laser fluence were plotted as a function of the square of partial pressure ratios of $[Tol]^2/[Bz]^2$ in the beam. The slope of the fitted straight line is 8.6 ± 0.3, corresponding to $(k_{VT-T}/k_{VB-B})(k_{Tol}/k_{Bz})$ as described in eq 10. Hence, k_{VT-T}/k_{VB-B} becomes 2.1 ± 0.4 and the second toluene toward $V_1(C_6H_5CH_3)_1$ is about twice as reactive as the second benzene toward $V_1(C_6H_6)_1$.

Similarly, we measured the relative reactivity toward the V atoms between fluorobenzene and benzene to know effects of

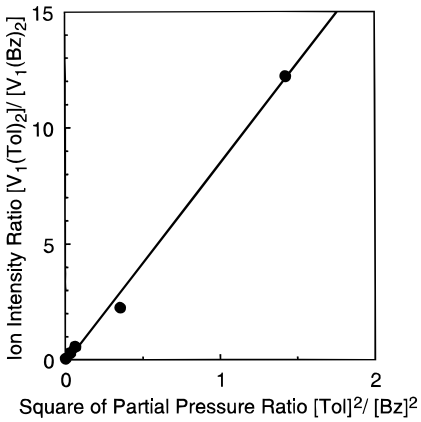

Figure 8. Plot of the ratios of ion intensities of $V_1(C_6H_5CH_3)_2$ to $V_1(C_6H_6)_2$ with normalization to the laser fluence vs the square of partial pressure ratios of $[Tol]^2/[Bz]^2$ in the beam. The slope of the fitted straight line gives 8.6 ± 0.3, corresponding to $(k_{VT-T}/k_{VB-B})(k_T/k_B)$ as indicated in eq 10 if ionization cross sections for $V_1(C_6H_5CH_3)_2$ and $V_1(C_6H_6)_2$ are equal (see text). Hence, k_{VT-T}/k_{VB-B} becomes 2.1 ± 0.4, and the second toluene is about twice as reactive as that of benzene toward a vanadium atom.

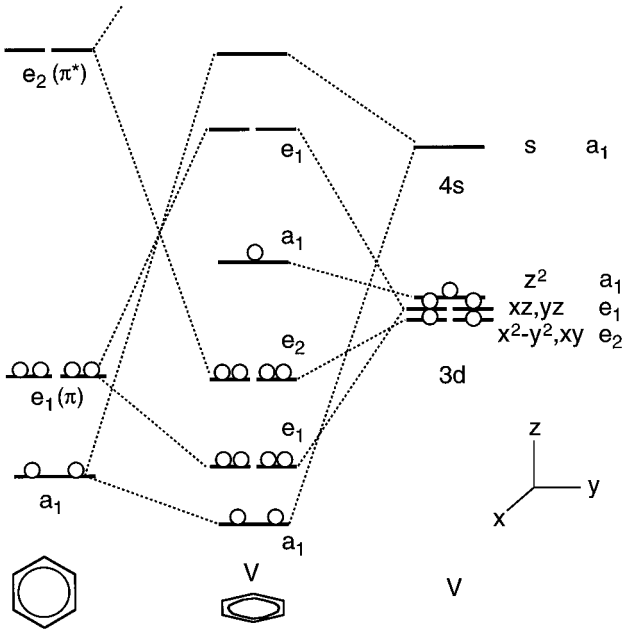

Figure 9. Schematic MO diagram of the valence orbitals in arene−V. Here, to compare $V_1(C_6H_6)_1$ with $V_1(C_6H_5CH_3)_1$, both these complexes are considered under the C_{6v} point group. Open circles indicate valence electrons.

electron-withdrawing ring substituents. The result was that fluorobenzene has a reactivity about 10^2 times as low as that of benzene in the production of $V_1(C_6H_5F)_2$. This corresponds to a very low yield in the synthesis of $V_n(C_6H_5F)_m$ compounds, as shown in the ArF mass spectra of $V_n(C_6H_5F)_m$ (Figure 1c).

As discussed above, it is concluded that an electron-donating ring substituent of toluene is more reactive than benzene, whereas an electron-withdrawing ring substituent of fluorobenzene has much less reactivity. To explain the higher reactivity of the toluene molecule, we make use of a molecular orbital (MO) diagram. The construction of the valence molecular orbitals in $V_1(\text{arene})_1$ is shown in Figure 9. Here, to compare $V_1(C_6H_6)_1$ with $V_1(C_6H_5CH_3)_1$, both orbitals of these complexes are considered under the C_{6v} point group symmetry. As shown in Figure 9, a metal $3d_{z^2}$ orbital of a_1 symmetry remains nonbonding. One of the benzene π sets of a_1 is stabilized by a metal 4s orbital, and the other benzene π sets of e_1 are stabilized by metal 3d orbitals (xz, yz) of e_1. The benzene π^* sets in e_2 symmetry are stabilized by metal $x^2 - y^2$ and xy of 3d orbitals (e_2). Thus, there are five strong bonding interactions between a vanadium atom and a benzene molecule. Among them, the main interaction is the overlap of e_1 symmetry orbitals. With methylation from benzene to toluene, E_i becomes lower (E_i = 9.25 eV for benzene and 8.82 eV for toluene, respectively[31]), and then the energy level of e_1 (π) orbitals becomes higher. Consequently, interaction between a toluene molecule and a vanadium atom becomes stronger, resulting in toluene having a higher reactivity than benzene toward vanadium. It is qualitatively reasonable that the reactivity of the first toluene molecule comes to be 4 times as high as that of benzene, and the second toluene has a reactivity twice as high as that of benzene, although the difference in reactivity of the second arene is a little smaller than that of the first arene. By use of this MO diagram, the reason why electron-donating ring substituents such as mesitylene (E_i = 8.41 eV[31]) exhibit high reactivity toward transition metal atom(s) can be figured out. It is the widespread view that alkyl substituted benzene stabilizes the metal−arene bonds[42] because the interaction between e_1 orbitals is expected to become stronger. For example, triple-decker sandwich compounds of $Cr_2(1,3,5\text{-}R_3\text{-benzene})_3$ (R = methyl and *tert*-butyl) have been prepared,[43] whereas $Cr_2(C_6H_6)_3$ has been not synthesized.[19]

The reason for the much lower reactivity of fluorobenzene molecules toward a vanadium atom cannot be explained by this qualitative MO diagram because the E_i of the fluorobenzene molecule is almost equal to that of benzene (9.25 and 9.21 eV for benzene and fluorobenzene, respectively[31]). Nevertheless, it is clear that the substitution of the hydrogen of benzene for an electron-withdrawing group decreases the reactivity for multiple-decker sandwich complex formation, and further theoretical investigation is necessary.

4. Conclusion

Organometallic clusters of $V_n(C_6H_5CH_3)_m$ and $V_n(C_6H_5F)_m$ were synthesized from the reaction between laser-vaporized metal atoms and arene molecules. $V_n(C_6H_5CH_3)_m$ clusters exhibited results similar to results of $V_n(C_6H_6)_m$ clusters in both mass distributions in the mass spectra and ionization energies, which leads us to conclude that $V_n(C_6H_5CH_3)_m$ takes the same sandwich structure as $V_n(C_6H_6)_m$. The relative reactivity between benzene and toluene toward vanadium atoms was also determined; electron-donating ring substitution of toluene enhances reactivity, in which toluene is about 4 and 2 times as reactive as benzene for the production of $V_1(\text{arene})_1$ and $V_1(\text{arene})_2$, respectively. On the other hand, the electron deficient arene of fluorobenzene has a much lower reactivity. We propose that the high reactivity of alkyl substituted benzene molecules depends on their lower ionization energy because the interaction between the e_1 orbitals of arene and vanadium atom becomes stronger.

Acknowledgment. We are very grateful to Dr. K. Hoshino, Mr. T. Kurikawa, Mr. H. Takeda, and Ms. N. Negishi for fruitful discussions. We are also grateful to Messrs. T. Yasuike and M. Gomei for valuable discussion from the theoretical point of view. This work is supported by a Grant-in-Aid for Scientific Research on Priority Areas from the Ministry of Education, Science, and Culture.

References and Notes

(1) Yeh, C. S.; Willey, K. F.; Robbins, D. L.; Pilgrim, J. S.; Duncan, M. A. *Chem. Phys. Lett.* **1992**, *196*, 233.

(2) Higashide, H.; Kaya, T.; Kobayashi, M.; Shinohara, H.; Sato, H. *Chem. Phys. Lett.* **1990**, *171*, 297.
(3) Holland, P. M.; Castleman, A. W. *J. Chem. Phys.* **1982**, *76*, 4195.
(4) Robels, E. S. J.; Ellis, A. M.; Miller, T. A. *J. Phys. Chem.* **1992**, *96*, 8791.
(5) Misaizu, F.; Sanekata, M.; Fuke, K.; Iwata, S. *J. Chem. Phys.* **1994**, *100*, 1161.
(6) Mitchell, S. A.; Blits, M. A.; Siegbahn, P. E. M.; Svensson, M. J. *Chem. Phys.* **1994**, *100*, 423.
(7) Larsen, B. S.; Ridge, D. P. *J. Am. Chem. Soc.* **1984**, *106*, 1912.
(8) (a) Jacobson, D. B.; Freiser, B. S. *J. Am. Chem. Soc.* **1985**, *107*, 1581. (b) Hettich, R. L.; Jackson, T. C.; Stanko, E. M.; Freiser, B. S. *J. Am. Chem. Soc.* **1986**, *108*, 1581.
(9) Nakajima, A.; Taguwa, T.; Hoshino, K.; Sugioka, T.; Naganuma, T.; Ono, F.; Watanabe, K.; Nakao, K.; Konishi, Y.; Kishi, R.; Kaya, K. *Chem. Phys. Lett.* **1993**, *214*, 22.
(10) Hoshino, K.; Kurikawa, T.; Takeda, H.; Nakajima, A.; Kaya, K. *J. Phys. Chem.* **1995**, *99*, 3053.
(11) (a)Kurikawa, T.; Hirano, M.; Takeda, H.; Yagi, K.; Hoshino, K.; Nakajima, A.; Kaya, K. *J. Phys. Chem.* **1995**, *99*, 16248. (b) Hoshino, K.; Kurikawa, T.; Takeda, H.; Nakajima, A.; Kaya, K. *Surf. Rev. Lett.* **1996**, *3*, 183.
(12) (a) *Structures and Dynamics of Clusters*; Kondow, T., Kaya, K., Terasaki, A., Eds.; Universal Academy Press: Tokyo, 1996; pp 129−134. (b) Kurikawa, T.; Takeda, H.; Nakajima, A.; Kaya, K. *Z. Phys. D.*, in press. (c) Kurikawa, T.; Takeda, H.; Hirano, M.; Judai, K.; Arita, T.; Nagao, S.; Yasuike, T.; Nakajima, A.; Kaya, K. *J. Phys. Chem.*, submitted.
(13) *Inorganic Chemistry*; Shriver, D. F., Atkins, P. W., Langford, C. H., Eds.; Oxford University Press: Oxford, 1990; pp 500−504.
(14) Lauher, J. W.; Hoffman, R. *J. Am. Chem. Soc.* **1976**, *98*, 1729.
(15) Zakin, M. R.; Cox, D. M.; Brickman, R. O.; Kaldor, A. *J. Phys. Chem.* **1989**, *93*, 6823.
(16) Irion, M. P.; Schnabel, P.; Selinger, A. *Ber. Bunsen-Ges. Phys. Chem.* **1990**, *94*, 1291.
(17) Irion, M. P.; Schnabel, P. *Ber. Bunsen-Ges. Phys. Chem.* **1992**, *96*, 1091.
(18) Yasuike, T.; Nakajima, A.; Yabushita, S.; Kaya, K. *J. Phys. Chem.*, in press.
(19) Muetterties, E. L.; Bleeke, J. R.; Wuchere, E. J.; Albright, T. A. *Chem. Rev. (Washington, D.C.)* **1982**, *82*, 499.
(20) (a) *Comprehensive Organometallic Chemistry*; Wilkinson, G., Stone, F. G. A., Abel, E. W., Eds.; Pergamon: New York, 1982; Vols. 3−6. (b) *Comprehensive Organometallic Chemistry II*; Abel, E. W., Stone, F. G. A., Wilkinson, G., Eds.; Pergamon: New York, 1995; Vols. 3−9.
(21) Wadepohl, H. *Angew. Chem., Int. Ed. Engl.* **1992**, *31*, 247.
(22) Braga, D.; Dyson, P. J.; Grepioni, F.; Johnson, F. G. *Chem. Rev. (Washington, D.C.)* **1994**, *94*, 1585.
(23) Green, M. L. H.; Ng, D. K. P. *Chem. Rev. (Washington, D.C.)* **1995**, *95*, 439.
(24) (a) Kealy, T. J.; Pauson, P. L. *Nature (London)* **1951**, *168*, 1039. (b) Miller, S. A.; Tebboth, J. A.; Tremaine, J. F. J. *Chem. Soc.* **1952**, 632.
(25) (a) Timms, P. L. *J. Chem. Educ.* **1972**, *49*, 782. (b) Skell, P. S.; Williams-Smith, D. L.; McGlinchey, M. J. *J. Am. Chem. Soc.* **1973**, *95*, 3337. (c) Klabunde, K. J.; Efner, H. F. *Inorg. Chem.* **1975**, *14*, 789. (d) Klabunde, K. J. *Acc. Chem. Res* **1975**, *8*, 393.
(26) *The Chemistry of the Metal-Carbon Bond*; Hartley, F. R., Patai, S., Eds.; John Wiley & Sons: New York, 1982; Vol. 1.
(27) Fischer, E. O.; Kögler, H. P. *Chem. Ber.* **1957**, *90*, 250.
(28) (a) Cloke, F. G. N.; Dix, A. N.; Green, J. C.; Perutz, R. N.; Seddon, E. A. *Organometallics* **1983**, *2*, 1159. (b) Andrews, M. P.; Mattar, S. M.; Ozin, G. A. *J. Phys. Chem.* **1986**, *90*, 744.
(29) Cloke, F. G. N.; Kahn, K.; Perutz, R. N. *J. Chem. Soc., Chem. Commun.* **1991**, 1372.
(30) Fischer, E. O.; Röhrscheid, F. *Z. Naturforsch., B* **1962**, *17*, 483.
(31) *Handbook of Chemistry and Physics*, 76th ed.; Lide, D. R., Eds; CRC Press: Boca Raton, FL, 1995; Section 6, p 77.
(32) *Structure and Bonding 43*; Goodenough, J. B., Hemmerich, P., Ibers, J. A., Jørgensen, C. K., Neilands, J. B., Reinen, D., Williams, R. J. P., Eds; Springer-Verlag: Berlin, 1981; pp 37−112.
(33) Klabunde, K. J.; Efner, H. F. *Inorg. Chem.* **1975**, *14*, 789.
(34) Cabelli, D. E.; Cowley, A. H.; Lagowski, J. J. *Inorg. Chim. Acta* **1982**, *57*, 195.
(35) Radonovich, L. J.; Zuerner, E. C.; Efner, H. F.; Klabunde, K. J. *Inorg. Chem.* **1976**, *15*, 2976.
(36) Elschenbroich, C.; Bilger, E.; Metz, B. *Organometallics* **1991**, *10*, 2923.
(37) Judai, K.; Hirano, M.; Kawamata, H.; Nakajima. A.; Kaya, K. *Chem. Phys. Lett.* **1997**, *270*, 23.
(38) Bowers, M. T. *Gas-Phase Ion Chemistry;* Academic Press: New York, 1979.
(39) *Handbook of Chemistry and Physics*, 76th ed.; Lide, D. R., Eds; CRC Press: Boca Raton, FL, 1995; Section 10, p 210.
(40) *Physical Chemistry*, 4th ed.; Atkins, P. W., Ed.; Oxford University Press: Oxford, 1990; p 161.
(41) Gomet, J. C. *Method. Phys. Anal.* **1967**, 71.
(42) Silverthon, W. E. *Adv. Organomet. Chem.* **1975**, *13*, 47.
(43) (a) Lamanna, W. M. *J. Am. Chem. Soc.* **1986**, *108*, 2096. (b) Lamanna, W. M.; Gleason, W. B.; Britton, D. *Organometallics* **1987**, *6*, 1583. (c) Cloke, F. G. N.; Courtney, K. A. E.; Sameh, A. A.; Swain, A. C. *Polyhedron* **1989**, *8*, 1641.